VOC GAS LEAK DETECTION USING PYRO-ELECTRIC INFRARED SENSORS

Fatih Erden[1], *E. Birey Soyer*[2], *B. Ugur Toreyin*[3], *A. Enis Çetin*[1]

[1]Dept. of Electrical and Electronics Eng., Bilkent University, Ankara, Turkey
[2]ASELSAN Inc., Ankara, Turkey
[3]Dept. of Computer Science and Engineering, University of Minnesota, MN

ABSTRACT

In this paper, we propose a novel method for detecting and monitoring Volatile Organic Compounds (VOC) gas leaks by using a Pyro-electric (or Passive) Infrared (PIR) sensor whose spectral range intersects with the absorption bands of VOC gases. A continuous time analog signal is obtained from the PIR sensor. This signal is discretized and analyzed in real time. Feature parameters are extracted in wavelet domain and classified using a Markov Model (MM) based classifier. Experimental results are presented.

Index Terms— VOC gas leak detection, pyro-electric infrared (PIR) sensor, wavelet transform, Markov Models

1. INTRODUCTION

Undesired release of combustible and toxic Volatile Organic Compounds (VOC) gases is an important problem as they are widely used in domestic and industrial life. In this paper, we propose a novel method for detecting and monitoring Volatile Organic Compounds (VOC) gas leaks by using a Pyro-electric (or Passive) Infrared (PIR) sensor which are widely used for motion detection in practice. To the best of our knowledge this is the first PIR based VOC gas detection system.

The main weakness of the conventional detectors is that the VOC gas vapor has to reach the sensor in order to be detected. Therefore, conventional detectors cannot provide quick responses in large rooms and open areas. The catalytic detector, commonly known as the "pellistor", is a combustible gas detector [1]. There must be at least 15% O_2 concentration in the environment for the sensor to work. The pellistor can be contaminated by the lead, silicone and certain other gases in the atmosphere, reducing the lifetime of the sensor [2]. Thermal conductivity (TC) gas detectors operate by comparing the conductivity of a sample gas with that of a reference gas, which is usually the air [2]. Semiconductor gas sensors have a similar operating principle. When gas vapour reaches the semiconductor gas sensor, it reacts with the oxide coating which changes the electrical conductivity due to an oxidizing reaction [3, 4]. The conductance of the device varies with the change in the atmospheric composition. O_2 concentration, temperature, humidity and exposure to silicone, sulphur compounds may have significant effect on the sensitivity of the detector. When the VOC gas vapor reaches an electrochemical gas sensor through the membrane by diffusion, oxidation reaction occurs and this causes an electrical current proportional to gas concentration [5]. Similar to the catalytic sensors, electrochemical gas sensors also suffer from atmospheric contaminants and extreme hot and cold temperatures. They can not be used in places containing more than 25% CO_2 [2]. Another class of sensors include a laser-supported technique for measuring CO concentration [6]. A laser diode emits infrared light with an absorbtion wavelength of the VOC gas vapor. The beam is attenuated whenever there is gas vapor in the container. They are expensive because of the laser. The vapor has to reach the sensor as the other conventional systems.

In this paper, the use of pyro-electric infrared (PIR) sensor for VOC gas leak detection is described. PIR sensors can be used open areas. Since, they generate a voltage proportional to the incident infrared radiation power, it is not necessary for the vapor to reach the sensor. It is sufficient for the gas to be in the viewing range of the PIR device. The main advantage of the PIR sensor based VOC gas detection system over the conventional sensors is its almost instantaneous response time, it does not get contaminated by the the contaminants in the atmosphere, it does not require the existance of certain amount of 02 in the environment, and its extremely low-cost. A continuous-time analog signal is obtained from the PIR sensor by modifying the sensor circuitry. This signal is discretized and analyzed in real time by using Markov Models (MM). Wavelet coefficients are used as feature parameters by Markov models. Section 2 describes the modified PIR sensor circuit. The MM-based decision engine is described in Section 3. Experimental results are presented in Section 4.

2. DATA ACQUISITION FROM THE PIR SENSOR

Commercial PIR sensor circuits produce binary outputs. A circuit is developed to extract a continuous time analog signal from the sensor [7]. The block diagram of the circuit is shown in Figure 1. The circuit captures a signal representing

A. E. Çetin is on leave at Dept. of Electrical Engineering, Ryerson University, Toronto, Canada. This work is partially supported by EC-FP7-FIRESENSE project and TUBITAK

the strength of the received signal as a function of time. The sensor output signal is fed into a two stage amplifier and digitized by using a PIC16F877A-type microcontroller device. Resulting discrete-time signal can be processed using a digital signal processor or a general purpose computer. The analog signal is sampled with a sampling frequency of f_s=100 Hz, which is sufficient to capture a VOC gas leak. A typical sampled signal for 'no activity' case using 8 bit quantization is shown in Figure 2. The non-zero mean value of this signal is mainly due to the background room temperature. Figure 3 shows the PIR output signal due to a walking person and a gas leak event at a distance of 1 m. In Figure 3(a), there is no activity up to 33^{rd} second and there is a walking person in the viewing range of the PIR sensor between 33 and 40 seconds. There is no activity again up to 87th second and there is another walking activity. In Figure 3(b), a VOC gas leak at 53^{rd} second is presented, after a 'no activity' case. The VOC gas leak event actually continues up to the end of the record, but after some time the observed output signal behaves as if it belongs to a 'no activity' event. This is because PIR sensors give an electric response to the rate of change of IR radiation rather than the temperature or IR radiation itself. As a result the sensor updates its background level when the same event continues to happen in its viewing range for some time.

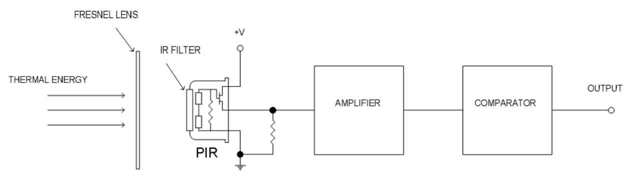

Fig. 1. The circuit diagram for capturing an analog signal output from a PIR sensor.

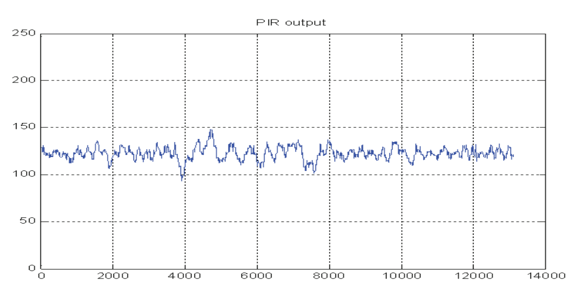

Fig. 2. A typical background PIR sensor output signal sampled at 100 Hz with 8 bit quantization when there is 'no activity' in its viewing range.

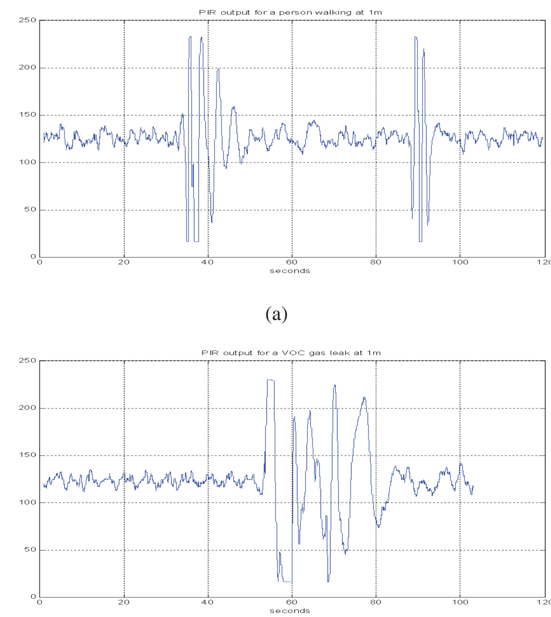

(a)

(b)

Fig. 3. PIR sensor output signals recorded at a distance of 1m for (a) a walking person and (b) for a VOC gas leak. Sampling frequency is 100 Hz.

3. SENSOR DATA PROCESSING

The strength of the PIR sensor output signal increases or decreases due to hot body actions in its viewing range and the analysis is made by using these changes. Therefore, any changes in the temperature of the room or IR absorption or illumination, where PIR sensor is placed, affect the analysis. Slow temperature changes cause a bias in the output of the sensor. To remove this bias and slow down the variations, the discrete wavelet transform (DWT) is used as a feature extractor [8], [9]. DWT also reduces the amount of data to be processed by Markov models.

Let $x[n]$ be a sampled version of the PIR sensor signal and $d_i[n]$ be the i-th level wavelet coefficients, which are obtained after a multirate subband decomposition process. The Daubechies wavelet filter bank is used in the analysis. A single stage DWT is computed by successive half-band low-pass and high-pass filtering of the signal followed by downsampling by a factor of two. At each level the high pass filter produces the detail signal, $d_i[n]$, while the low pass filter associated with scaling function produces coarse approximations, $a_i[n]$, i=1,2,3,4. In this analysis, a four-stage decomposition is used to obtain the wavelet coefficients $d_i[n]$, i=1,2,3,4. The wavelet coefficients $w[n] = d_4[n]$ of the VOC gas leak signal in Figure 3(b) is shown in Figure 4. Due to downsampling, after a four-stage WT, 6.25 samples correspond to 1 second while 100 samples correspond to 1 second in the original data.

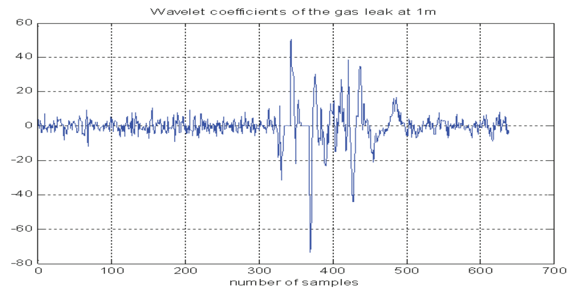

Fig. 4. Wavelet coefficients of the PIR sensor output signal recorded at a distance of 1m for the VOC gas leak shown in Figure 3(b).

Markov Modeling: Once the wavelet coefficients are obtained, a MM based classification procedure, similar to the one in [7], is carried out for VOC gas leak detection. There are three types of events to be classified: a walking person, a gas leak and a no-activity event. Two three-state Markov models are used to model a VOC gas leak and a walking person. In the training step, two threshold values are defined in the wavelet domain for each model, $T_1 < 0$ and $T_2 > 0$. Since the wavelet signal is a zero mean signal, $T_2 = -T_1$. The same threshold values are used in each model. Let the three states be S_0, S_1 and S_2. States of wavelet coefficients are defined as follows:

if $(w[k] < T_1)$
then state S_0
else if $(T_1 < w[k] < T_2)$
then state S_1
else
state S_2 is attained accordingly
end

Thresholds are defined such that the wavelet coefficients of the no-activity event remain in state S_1. The system is in state S_1 as long as there is not any significant activity in the viewing range of the PIR sensor. Therefore, although there are three events to be classified, only two Markov models are used, one for a walking person and the other for a gas leak as shown in Figure 5. No-activity event is detected by controlling whether the system remains in S_1 or not.

During the training phase, only the state transition probabilities $p_a(i, j)$ and $p_b(i, j)$ are estimated for each model. During the classification process, we only use two models corresponding to the VOC gas leak and walking person events as the system mostly remains in state S_1 when there is no activity, the state transition probability, $p(1, 1)$, is very close to 1 and others are close to 0. To decide the class affiliation of a test signal, state vector and the corresponding number of

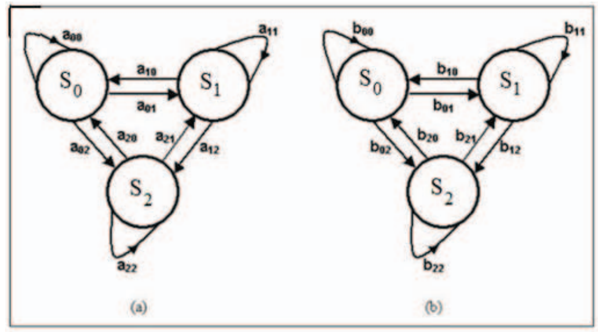

Fig. 5. Markov models and state transition definitions for (a) 'VOC gas leak' and (b) 'walking person' classes.

transitions of the signal are determined. Let C be the state sequence of the test signal and t_{ij} be the number of transitions from $i - th$ state to $j - th$ state. Then the probabilities for the state sequence C of belonging to 'gas leak' and 'walking person' classes are computed as follows:

$$P_{a,b}(C) = \prod_{i=1}^{L} p_{a,b}(C_{i+1}|C_i) = \prod_{i=0}^{2}\prod_{j=0}^{2} (p_{a,b}(i,j))^{t_{ij}}, \quad (1)$$

where L is the length of the state sequence C of the test signal. During the classification phase, the state sequence of the test signal C is divided into windows of length 25 and each window is fed into the 'gas leak' and the 'walking person' models. The model yielding the highest probability is determined and monitored at the end of each 4 seconds period, as the result of the analysis of PIR sensor data. To avoid multiplications during classification, we use Eq. 2 instead of Eq. 1.

$$P'_{a,b}(C) = \sum_{i=0}^{2}\sum_{j=0}^{2} t_{ij} \log_{10}(p_{a,b}(i,j)) \quad (2)$$

Log values are obtained from a look-up table. The decision algorithm is as follows:

if $P_a(C) > P_b(C)$
then the test window is affiliated with the 'gas leak' class
else
the window is affiliated with the 'walking person' class
end
if $p_{test}(1, 1) > 0.8$
the test window is affiliated to the 'no-activity' class
end

4. EXPERIMENTAL RESULTS

The detection range of the PIR sensor is 5 meters, but in our experiments we record VOC gas leak and walking person sequences at a distance of up to 3 meters because we use the

PIR sensor without the Fresnel lens on it. As a result, after 3 meters the strength of the PIR output signal decreases and the sensor is not able to respond to the changes. We used a bottled gas which contains a mixture of butane and propane gases, in ratios of %70 and %30, respectively. We recorded the VOC gas leak signal by releasing gas vapor from the container when it is 10 cm, 1 meter and 3 meters away from the sensor. We first started recording the background and then start the VOC gas leak without entering the viewing range of the sensor. In 4 of 32 gas leak experiments, we used a 1 meter long pipe between the sensor and the bottled gas to have controlled experiments making sure that the sensor signal is due to the gas vapor.

Since the PIR sensor also reacts to the ordinary motion of hot bodies, we recorded signals due to a person walking in the viewing range of the PIR sensor on a straight line which is tangent to a circle with a radius of 1, 2 and 3 meters and the sensor being at the center. We also record waving arm movements at distances of 1, 2 and 3 meters to the sensor.

We use the threshold values, ($T_1 = -T_2 = 10$) to estimate the reference transition probabilities. Threshold values are greater than 2.5σ of the background signal. The state sequence is divided into windows of lengths 25, each covering a time frame of 4 seconds. At the end of each time frame, the result of the analysis is monitored. If two consequent frames are analyzed as gas leak, we trigger an alarm. Moreover, if the probability of a transition from S_1 to S_1, $p_{test}(1,1)$, is greater than 0.8, we decide that there is no-activity. The results for the MM analysis are presented in Table 1. Our method successfully detects VOC gas leak for 30 of the 32 gas leak test sequences. The two missed leaks belong to cases that are at a distance greater than 3 meters to the sensor. The strength of the output signal of the PIR sensor decreases for the leaks far away from the sensor and they are analyzed as a no-activity event. Our system triggers a false alarm for 5 of 50 non-gas test sequences. Three of them belong to the walking person and two of them belong to the arm waving experiments. If a person is at a distance of up to 1m, we do not encounter any false alarms. However, when the person is far away, the strength of the sensor output signal decreases, as a result walking event may be confused as a gas leak. Therefore, the range of our VOC sensor is 1 meter and it can be placed facing valves and other possible leak locations.

Table 1. Classification results for 32 VOC gas leak and 50 non-gas test sequences. The system triggers an alarm when a VOC gas leak is detected in the viewing range of the PIR sensor.

Test Seq.	# of Test Sequences	# of False Alarms	# of Missed Leaks	# of Detect.
Gas Leak	32	-	2	30
Non-Gas	50	5	-	-

We also carried out experiments with different sensors. For example, a ME-O2 electrochemical gas sensor has a response time of about 30 seconds [10], a MQ-4 gas sensor has a response time longer than 5 minutes [11] and a hydrogen-selective gas sensor described in [12] has a response time of 50 seconds. On the other hand, we can detect a gas leak with a PIR sensor at 8 seconds.

5. CONCLUSION

In this study, we proposed and implemented a novel and cost efficient method for VOC gas detection by using a PIR sensor. We used the fact that the sensor has spectral response in the infrared part of the spectrum intersecting with the absorption bands of butane and propane gases. Gas vapor spread out gradually, whereas the IR radiation propagation is very rapid. Therefore, unlike conventional detectors, infrared sensor has fast response time.

Markov models (MM) which are tailored for VOC gas detection are used and they process the wavelet transformed sensor data. The algorithm is computationally efficient and it can be implemented using a low-cost digital signal processor.

6. REFERENCES

[1] J. G. Crowder, S. D. Smith, A. Vass, and J. Keddie, *Mid-infrared Semiconductor Optoelectronics*, chapter Infrared Methods for Gas Detection, pp. 595–613, Springer Berlin / Heidelberg, 2006.

[2] Cambridge Sensotec, "Gas analysis methods," `http://pdf.directindustry.com/pdf/cambridge-sensotec/gas-detection-methods-explained/14678-44117-42.html`, Accessed at May 2009.

[3] D.D. Lee and D.S. Lee, "Environmental gas sensors," *Sensors Journal, IEEE*, vol. 1, no. 3, pp. 214–224, Oct 2001.

[4] Figaro Engineering Inc., "Tgs 2610 - for the detection of lp gas," .

[5] E. Bakker and M. Telting-Diaz, "Electrochemical sensors," *Anal. Chem.*, vol. 74, 2002.

[6] N. Aschenbrenner, "Laser diode measures carbon monoxide traces," `http://w1.siemens.com/innovation/en/news_events/ct_pressemitteilungen/index/e_research_news/2009/e_22_resnews_0901_1.htm`, Accessed at May 2009.

[7] B.U. Töreyin, E.B. Soyer, O. Urfalioglu, and A.E. Cetin, "Flame Detection System Based on Wavelet Analysis of PIR Sensor Signals with an HMM Decision Mechanism," in *16th European Signal Processing Conference (EUSIPCO 2008)*, 2008.

[8] Yuan Y. Tan, *Wavelet Theory and Its Application to Pattern Recognition (Machine Perception & Artificial Intelligence)*, World Scientific Publishing Company.

[9] E. Bala and A.E. Cetin, "Computationally efficient wavelet affine invariant functions for shape recognition," vol. 26, no. 8, 2004.

[10] Hanwei Electronics, "ME-O2 Electrochemical Gas Sensor," `http://www.diytrade.com/china/4/products/5010173/O2_electrochemical_gas_sensors.html`, Accessed at May 2009.

[11] Hanwei Electronics, "Technical Data MQ4 Gas Sensor," `http://www.hwsensor.com/English/PDF/sensor/MQ-4.pdf`, Accessed at May 2009.

[12] Woosuck Shin, Masahiko Matsumiya, Noriya Izu, and Norimitsu Murayama, "Hydrogen-selective thermoelectric gas sensor," *Sensors and Actuators B: Chemical*, vol. 93, no. 1-3, pp. 304 – 308, 2003, Proceedings of the Ninth International Meeting on Chemical Sensors.